Preparation of Liquid-Core Nanocapsules from Poly[(ethylene oxide)-*co*-glycidol] with Multiple Hydrophobic Linoleates at an Oil−Water Interface and Its Encapsulation of Pyrene

Yong Ren, Guowei Wang, and Junlian Huang*

Key Laboratory of Molecular Engineering of Polymers, State Education Ministry of China, Department of Macromolecular Science, Fudan University, Shanghai 200433, China

Received February 14, 2007; Revised Manuscript Received April 4, 2007

A convenient approach is provided to prepare liquid-core nanocapsules by cross-linking an amphiphilic copolymer at an oil−water interface. The hydrophilic copolymer poly[(ethylene oxide)-*co*-glycidol] was prepared by anionic polymerization of ethylene oxide and ethoxyethyl glycidyl ether first, then the hydroxyl groups on the backbone were recovered after hydrolysis and partly modified by hydrophobic conjugated linoleic acid. The copolymer with multiple linoleate pendants was absorbed at an oil−water interface and then cross-linked to form stable nanocapsules. The mean diameter of the nanocapsule was below 350 nm, and the size distribution was relatively narrow (<0.2) at low concentrations of oil in acetone (<10 mg/mL). The particle size could be tuned easily by variation of the emulsification conditions. The nanocapsule was stable in water for at least 5 months, and the shell maintained its integrity after removal of the oily core by solvent. Pyrene was encapsulated in these nanocapsules, and a loading efficiency as high as 94% was measured by UV spectroscopy.

Introduction

Poly(ethylene oxide) is one of the most popular biocompatible polymers. It possesses an ideal array of properties:[1] very low toxicity, excellent solubility in aqueous solutions, extremely low immunogenicity and antigenicity. PEO also exhibits excellent pharmacokinetic and biodistribution behaviors. When injected into animals it shows high persistence in the blood and low accumulation in reticuloendothelial system (RES) organs, liver, and spleen. It has the propensity in vivo to exclude proteins, other macromolecules, and particulates from its surroundings. These properties of PEO have been attributed to its high chain mobility associated with conformational flexibility and water-binding ability.[2,3]

A major limitation facing the intravenous delivery of polymeric nanocapsules is their rapid elimination from systemic circulation by blood monocytes and cells of the mononuclear phagocyte system (MPS).[4] Long-circulating, "stealth" carriers are generally obtained by grafting PEO at the carrier surface.[5] The modification of nanoparticles with PEO leads to a longer half-life in blood circulation. Hoarau[6] et al. reports that PEGylated lipid nanocapsules exhibited long-circulating properties. Up to 50% of the injected dose was still present in the blood 8 h after administration for lipid nanocapsules containing 6 mol % PEO 5000 or 10 mol % PEO 2000. Mosqueira[7] et al. demonstrates that covalent attachment, longer PEO chain lengths, and higher densities are necessary to increase the circulation half-life of PEO surface-modified poly(*rac*-lactide) nanocapsules in vivo.

Polymer capsules having a polymeric shell and a liquid core offer versatility for encapsulation and controlled delivery of drugs, dyes, enzymes, and many other substrates.[8−12] They are vesicular systems in which the drug is confined to a cavity surrounded by a single polymeric membrane and better protected during storage and after administration. Compared with ordinary micelles, as nanocontainers or nanoreactors, they are expected to have a much higher efficiency of encapsulation, particularly for large-size molecules.[13] These important applications have driven the rapid development of innovative techniques such as interfacial polymerization or polycondensation,[14−18] shell polymerization or cross-linking of particles followed by core removal,[19] internal phase separation from miniemulsions,[20] and self-assembly of block copolymers.[21,22]

Amphiphilic copolymers are unique building blocks in supramolecular polymer chemistry, and their variable properties, structures, and molecular weights of the polymer blocks make it possible to design nanomaterials with specific functions. Polymer capsules can be prepared by either cross-linking the shell of core−shell micelles of amphiphilic copolymer and then removing the core or directly forming double-layer vesicles. There are numerous works on these two methods,[23,24] but only a few reports have reported liquid-core capsules directly prepared by cross-linking amphiphilic copolymers at an oil−water interface. In fact, amphiphilic copolymers are useful for mediation of an oil−water interface, as demonstrated by its rich science and commercial utility as a polymer surfactant. Emrick et al.[25] reported polymer capsules prepared by ring-opening cross-metathesis of self-assembled amphiphilic PEO-grafted polyolefins at the toluene−water interface. Stöver et al.[26] developed a technique for preparing capsules with a diphenyl ether core. They prepared poly[methyl methacrylate-*co*-poly(ethylene glycol) methacrylate] oligomers in diphenyl ether solution first to which a monomer used as a cross-linking agent was added, and then this oil phase was transferred to a stirred aqueous phase to prepare capsules. These two capsules described above are all larger than 10 μm. However, for more and more applications, especially in medicine, smaller capsules between 50 and 300 nm are of high interest.[14] For example, the capsules (<1 μm), which are called nanocapsules, have the advantage that can be administered intravenously without any risk of embolization.[13]

* Author to whom correspondence should be addressed. E-mail: jlhuang@fudan.edu.cn.

10.1021/bm0701797 CCC: $37.00
Published on Web 05/23/2007

We have developed a new methodology to prepare liquid-core nanocapsules with a hydrophilic PEO surface. The nanocapsules are smaller than 350 nm. Our approach involves the following steps: (1) The hydrophilic polymer was modified by hydrophobic molecules; (2) the obtained amphiphilic polymers were cross-linked at an oil−water interface. In our experiment, poly[(ethylene oxide)-*co*-glycidol] copolymer was used as the hydrophilic polymer.

The modification of hydrophilic polymer with hydrophobic molecules is a very easy operation. A broad range of common hydrophilic polymers such as poly(acrylic acid), polyvinylpyridine, and poly(vinyl alcohol) can be easily modified and then used to prepare liquid-core nanocapsules. Thus this method provides significant opportunity to reach a large number and diverse range of functionalities in terms of the properties of the backbone and the grafted molecules.

The nanocapsules described in this article are expected to be useful in drug delivery because of the small particle size and the hydrophilic PEO surface. Furthermore, the residual hydroxyl groups on the backbone also provide the possibility for further modification of the capsules.

Experimental Section

Materials. Glycidol (technical grade) was purchased from Acros, dried over calcium hydride for 48 h, and then distilled under reduced pressure just before use. Glycidol protected with ethyl vinyl ether (ethoxyethyl glycidyl ether, EEGE) was produced according to the procedure described by Fitton et al.[27] Triethylene glycol (TEG) was distilled from CaH_2 under reduced pressure. Ethylene oxide (EO) (Sinopharm Chemical Reagent Co., Ltd., 98%) was dried by calcium hydride for 48 h and then distilled under N_2 before use. Conjugated linoleic acid (a mixture of *cis*- and *trans*-9,11- and -10,12-octadecadienoic acids, 90%) was purchased from Qingdao Aohai Biotechnologies Co., Ltd., and used as received. Octadecane (OD), hexadecane, undecane, and heptane were purchased from Sinopharm Chemical Reagent Co., Ltd., and used without further purification.

Measurements. ^{1}H NMR spectra were obtained on a DMX 500 MHz spectrometer, using $CDCl_3$ as the solvent. UV absorption spectra were obtained with a 756 MC UV−visible spectrophotometer (Shanghai Third Analytical Instrument Factory, China). IR spectra were obtained on a Magna-550 Fourier transform infrared spectrometer. The surface tension of the miniemulsion was measured by a JYW-200A tensiometer from Chengde Instrument Factory at 20 °C. Size exclusion chromatography (SEC) was performed on an Agilent 1100 with a G1310A pump, a G1362A refractive index detector, and a G1314A variable-wavelength detector with tetrahydrofuran (THF) as the eluent at 35 °C. Dynamic light scattering (DLS) measurements were performed at 30 °C on a Malvern Autosizer 4700 dynamic light scattering instrument. Transmission electron microscopy (TEM) was performed on a Hitachi H-600 microscope at an accelerating voltage of 75 kV. The specimens were prepared by depositing 10 μL of nanocapsule dispersions on carbon-coated grids. The samples were left to dry in the air for 1 h before imaging. Atomic force microscopy (AFM) imaging was performed in tapping mode on a Nanoscope IV from Digital Instruments. A tapping tip was used (tip curvature radius, <10.0 nm), and the amplitude setpoint was 1 V. The sample preparation was similar to that for TEM, but mica was used as a substrate. The ultrafiltration membrane separator was purchased from the Shanghai Institute of Nuclear Research, Chinese Academy of Sciences. The cutoff molecular weight of the poly(ether solfone) film was 20 kDa (calibrated by a global protein).

Anionic Copolymerization of EEGE with EO. The copolymerization equation of EEGE with EO is shown in Scheme 1, and the complete reaction was described in a previous publication.[28] Diphenylmethyl potassium (DPMK) was prepared first as follows: to a 150 mL three-necked flask, 100 mL of dry THF and 7.7 g (0.06 mol) of naphthalene were added, and then 2.34 g (0.06 mol) of potassium with a fresh surface was added under a nitrogen atmosphere. After 4 h of stirring, 11.1 g (0.066 mol) of diphenylmethane was introduced with a syringe, and the system was refluxed at 80 °C for 24 h and titrated with 0.1 M HCl after filtration. The concentration of DPMK was 0.57 mol/L. The copolymerization was carried out in a kettle. A 150 mL kettle was vacuumed at 80 °C for 2 h and cooled to room temperature and then to −20 °C. A given volume of initiator solution (TEG (0.67 mL, 0.005 mol) and DPMK (3.5 mL, 0.002 mol) in 50 mL of THF), EEGE (20 g, 0.14 mol), and EO (50 g, 1.14 mol) were introduced successively into the kettle under magnetic stirring. Then it was heated to 60 °C under stirring for 48 h. The reaction was terminated by the addition of a few drops of acidified methanol. After all of the solvents were removed, the crude product was dissolved in CH_2Cl_2, dried over anhydrous $MgSO_4$, and filtered. A yellowish, viscous product poly(ethylene oxide-*co*-2,3-epoxypropyl-1-ethoxyethyl ether) (poly(EO-*co*-EEGE)) was obtained in a yield of 94% after CH_2Cl_2 was removed. The obtained copolymer was characterized by ^{1}H NMR and SEC. The molar ratio of EEGE to EO in the copolymer was determined by ^{1}H NMR. Characterizaiton: δ = 4.63−4.75 ppm [−O−C*H*(CH$_3$)−O−], δ = 1.30, 1.29 ppm (−O−CH(C*H*$_3$)−O−), δ = 1.21, 1.19, 1.18 ppm (−O−CH$_2$C*H*$_3$), δ = 3.53−3.80 ppm [−O−C*H*$_2$CH$_3$, −OC*H*$_2$C*H*$_2$O−, and −OC*H*$_2$C*H*(C*H*$_2$OH)O−].

Scheme 1. Preparation of Ethylene Oxide and Glycidol Copolymer

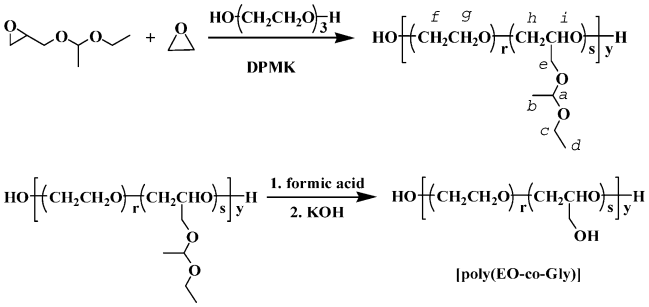

Hydrolysis of the EEGE Units of poly(EO-*co*-EEGE). The hydrolysis of poly(EO-*co*-EEGE) was carried out as previously described in the literature.[28] Briefly, 10.0 g of poly(EO-*co*-EEGE) (M_n 14.0 kDa, 0.7 mmol) was mixed with 160 mL of formic acid (0.27 mol), the solution was stirred at 20 °C for 30 min and evaporated under reduced pressure at 50 °C, the obtained product was dissolved in a mixture of dioxane (100 mL), methanol (50 mL), and KOH methanol solution (1 mol/L, 27 mL), and the solution was heated to reflux for 24 h and then neutralized with 5% HCl. After the solvents were removed under reduced pressure, the polymer was dissolved in water and purified by an ultrafiltration membrane separator. The pale yellow product, poly(ethylene oxide-*co*-glycidol) (poly(EO-*co*-Gly)), was obtained in a yield of 93%. The hydrolysis degree of the ethoxyethyl group was determined by ^{1}H NMR.

Esterification of poly(EO-*co*-Gly) with Conjugated Linoleic Acid. Poly(EO-*co*-Gly) (1 g) was dissolved in CH_2Cl_2 (30 mL), *N*,*N*-dicyclohexylcarbodiimide (DCC), dimethylaminopyridine (DMAP), and conjugated linoleic acid (CLA) were added, respectively, and the molar ratio of the reagents was CLA/copolymer/DMAP/DCC = 16:1:8:70. The reaction was carried out for 24 h at room temperature under nitrogen atmosphere. After the solvent was removed under reduced pressure, the crude product was dissolved in ethanol and purified by dialysis for 3 days. After the solvent was removed, the yellowish product (G2, Table 1) with a yield of 95% was obtained. The product was characterized by ^{1}H NMR and IR. The content of CLA was measured by UV absorption spectroscopy at 233 nm in ethanol ($\epsilon = 1.90 \times 10^4$ L mol^{-1} cm^{-1}).

Preparation of Liquid-Core Nanocapsules. The nanocapsules were prepared by dissolving PEO-CLA, CLA, hydrophobic oil, and azobisisobutryonitrile (AIBN, 0.5 mg) in 0.5 mL of acetone, and then the

Table 1. Composition of the Amphiphilic Graft Copolymer

sample code	$M_{n\ poly(EO\text{-}co\text{-}EEGE)}$ (kDa)	M_w/M_n[a]	R_T[b]	$M_{n\ poly(EO\text{-}co\text{-}Gly)}$ (kDa)	N_{OH}[c]	N_{CLA}[d]	P[e] (%)
G1	14.0	1.10	1/8.5	12.1	28.9	5.1	18
G2	14.0	1.10	1/8.5	12.1	28.9	8.0	28
G3	14.0	1.10	1/8.5	12.1	28.9	11.2	39
G4	14.0	1.10	1/8.5	12.1	28.9	18.9	65
G11	14.5	1.12	1/19.7	13.5	16.3	8.2	50

[a] The polydispersity of poly(EO-*co*-EEGE) as measured by SEC. [b] The ratio of EEGE-to-EO in the copolymer. [c] The number of hydroxyl groups on each polymer molecule. [d] The number of CLA side chains on each polymer molecule. [e] The percentage of reacted hydroxyl groups.

solution was poured into 10 mL of water under magnetic stirring at 30 °C for 24 h. After the dispersion was bubbled with nitrogen for 30 min, the temperature was elevated to 70 °C gradually. The cross-linking was performed at 70 °C for 24 h. The conversion of the diene group of CLA was estimated by UV spectroscopy. The particle sizes of the dispersions were characterized by dynamic light scattering. The morphologies of the capsules were determined by TEM and AFM.

Encapsulation of Pyrene. PEO-CLA, CLA, OD, AIBN (0.5 mg), and pyrene were dissolved in 0.5 mL of acetone, and then the obtained solution was poured into 10 mL of water under magnetic stirring at 30 °C. After the dispersion was bubbled with nitrogen for 30 min, the temperature was elevated to 70 °C gradually. The cross-linking was performed at 70 °C for 24 h. The dispersion was filtered through a 0.45 μm poly(tetrafluoroethylene) (PTFE) filter and then dissolved in acetone/water (v/v, 2:1). The concentration of pyrene was measured by UV absorption spectroscopy.

Results and Discussion

Synthesis of the Amphiphilic Copolymer. The copolymers of EO and glycidol (2,3-epoxypropanol-1) were prepared according to previous work[28] and described in the Experimental Section. The number of hydroxyl groups in poly(EO-*co*-Gly) was estimated according to the composition and the molecular weight of poly(EO-*co*-EEGE). The molar ratio of EEGE to EO in poly(EO-*co*-EEGE) was determined by ^{1}H NMR. The quartet at $\delta = 4.63-4.75$ ppm is assigned to the methyl protons (H_a) (Scheme 1) of the EEGE moiety, the doublet at $\delta = 1.30, 1.29$ ppm and the triplet at $\delta = 1.21, 1.19, 1.18$ ppm are assigned to methyl protons of the EEGE moiety (H_b and H_d), and the chemical shift at $\delta = 3.53-3.80$ ppm is assigned to the protons of the main chain (H_f, H_g, H_h, and H_i) and the protons of the lateral chains (H_c, H_e). The copolymer composition can be readily obtained by eq 1 based on the ^{1}H NMR spectrum

$$R_T = \frac{4A_a}{A_{sum} - 7A_a} \quad (1)$$

where R_T is the molar ratio of EEGE to EO in the copolymers, A_{sum} represents the peak area sum of protons c, e, f, g, h, and i, and A_a represents the peak areas of the methine protons of the EEGE moiety.

Poly(EO-*co*-Gly) is then obtained by hydrolysis of poly(EO-*co*-EEGE), and all of the peaks of H_a, H_b, and H_d for the EEGE unit in NMR disappeared, which meant that the acetal groups of poly(EO-*co*-EEGE) are cleaved completely. SEC also confirmed that the hydrolysis did not affect the main chain of the copolymer, since no change is found for molecular weight distribution of the copolymers. The number of hydroxyl groups on poly(EO-*co*-Gly) was calculated according to eq 2

$$N_{OH} = \frac{M_n - 18}{44 + 146R_T} \times R_T + 2 \quad (2)$$

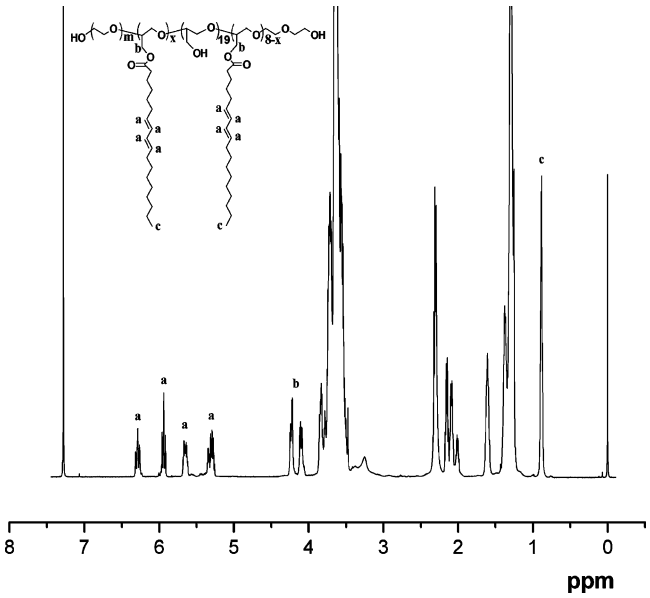

Figure 1. ^{1}H NMR spectrum of amphiphilic graft copolymer G2 ($m = 229$, $x = 0-8$).

Here N_{OH} is the number of hydroxyl groups in each molecule of poly(EO-*co*-Gly) and M_n is the number-average molecular weight of poly(EO-*co*-EEGE) measured by SEC. R_T has the same meaning as in eq 1. In this presentation, two poly(EO-*co*-Gly) copolymers with molecular weights of 12.1 and 13.5 kDa (hydroxyl numbers, 28.9 and 16.3, respectively) are used (Table 1).

Conjugated linoleic acid is coupled with the hydroxyl groups of the copolymer in the presence of ′DCC and DMAP at room temperature. Characterization of the copolymer with CLA side chains (PEO-CLA) is achieved by ^{1}H NMR (Figure 1) and IR. The peaks at 4.1−4.3 ppm in ^{1}H NMR and the absorption at 1736 cm^{-1} in IR spectra indicated the formation of the ester bond. The content of CLA is determined by UV absorption at 233 nm. The compositions of the obtained amphiphilic copolymers are listed in Table 1.

Influence of the Oil Concentration in Acetone on Miniemulsions. Miniemulsions are dispersions of relatively stable oil droplets with a size range of 50−500 nm in water, generally prepared by shearing a system containing oil, water, surfactant, and costabilizer (or hydrophobe).[14] High-shear devices are commonly used to break up the dispersed phase into submicron droplets. Here we used the spontaneous droplet formation method, which is named the ouzo effect,[29] to prepare miniemulsions. Vital and Katz[30] have reported the preparation of a metastable liquid dispersion by homogeneous liquid−liquid nucleation. The spontaneous emulsification occurs upon pouring, into water, a mixture of totally water miscible solvent and hydrophobic oil, thus generating long-lived small droplets, which are formed even though no surfactant is present.

The copolymer G3 with a concentration being equal to 10 wt % of OD was used to investigate the effect of OD concentration in acetone on the miniemulsion. The OD concentration in acetone varied from 1.3 to 16 mg/mL. Figure 2 shows the particle diameters and polydispersities of the obtained miniemulsions, from which it is observed that as the concentration of OD in acetone increases the diameter of the particle increases linearly. Katz described in his article that the mean droplet diameter of the dispersion produced by the ouzo effect is a linear function of the excess oil-to-solvent ratio. On mixing with water, the oil becomes greatly supersaturated, which results

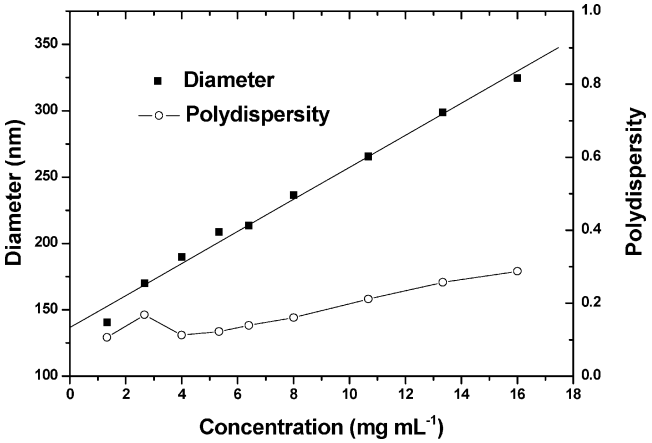

Figure 2. Mean droplet diameter and polydispersity of the miniemulsion as a function of OD concentration in acetone. (The method of Contin analysis was used to estimate the polydispersity of the droplets.)

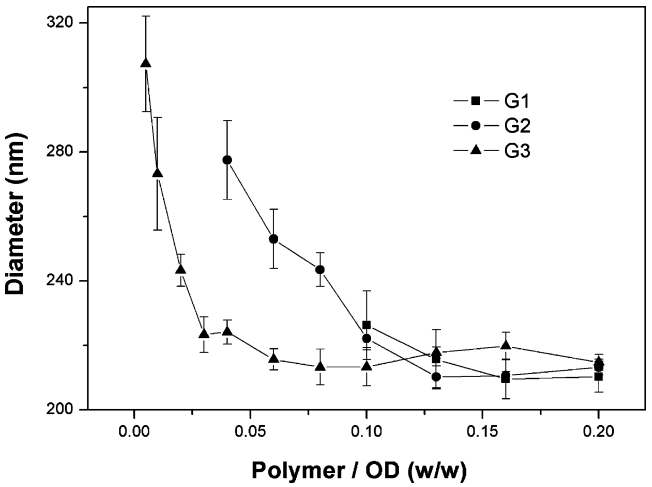

Figure 3. Mean droplet diameter of the miniemulsion as a function of the polymer-to-OD ratio. (The error bar shows the standard deviation of the particle size.)

in the nucleation of oil droplets, and then oil immediately diffuses to the nearest droplet, so the supersaturation is alleviated and no further nucleation occurs. In a solution with low oil-to-acetone ratios, oil molecules near each nucleus are so few that only very small droplets form. Conversely, with an increasing oil-to-solvent ratio, more oil molecules are near to the nucleus, so large droplets are formed. Our results are in agreement with the Katz's conclusion, which means that the size of the particle can be tuned by varying the concentration of oil in acetone. From the polydispersity curve it can be found that the size distributions of the particles are relatively narrow, especially at a low concentration of OD.

When the concentration OD in acetone is above 20 mg/mL, large droplets are formed and then coalesced rapidly, so it is unsuitable to prepare stable dispersions at a high concentration OD in acetone.

Influence of the Polymer-to-Oil Ratio on Miniemulsions. Amphiphilic copolymers G2 and G3 are used to examine the influence of the polymer-to-oil ratio on miniemulsions, and OD is used as the hydrophobic oil. The ratio is varied from 0.5:100 to 20:100 while the concentration of OD in acetone is kept at 6.4 mg/mL. From the curve of G3 in Figure 3 it is found that the diameter of the droplet increased rapidly with the decrease of the polymer-to-oil ratio from 6:100 to 0.5:100. But when the ratio is larger than 8:100, the diameter of the droplet is no

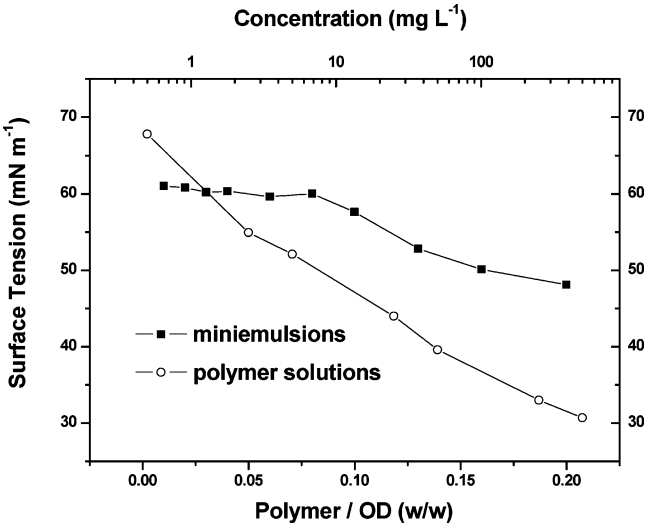

Figure 4. Surface tension as a function of the G3-to-OD ratio or G3 concentration in solution.

longer varied much and only fluctuated at 210 nm, which means that the amount of the polymer does not affect the size of the droplets at a high polymer-to-oil ratio. The curve of G2 also gives a similar result.

In miniemulsions generated by high-shear devices such as a sonicator, the size of the droplets directly depends on the amount of surfactant. The diameter of the droplets is decreased as the amount of the surfactant is increased. However, in our cases, the diameter of the droplet is no longer varied at a high polymer-to-oil ratio, so how do we explain this phenomenon? We think that in the miniemulsion prepared with a sonicator the fusion−fission rate would maintain equilibrium during sonication, and more surfactant would decrease the fusion rate, then leading to smaller droplets. In our experiment, however, there are two processes to form a stable droplet. First, the oil droplets are formed immediately after acetone diffuses into water, and then the polymer is absorbed at the oil−water interface to prevent the droplets from coalescing. From the curve of G3 we can deduce that when the G3-to-oil ratio is smaller than 6:100 the polymer is not sufficient to protect the smallest droplets formed by the first process (ca. 210 nm), so the coalescence of the droplets into larger ones and the increase of the particle size are unavoidable. When the ratio is larger than 8:100, the polymer is sufficient to prevent the droplets from coalescing, the particle size is merely determined by the first process, and the amount of polymer does not affect the size of the oil droplets anymore.

To verify this explanation, the surface tension of the miniemulsions prepared with G3 was measured. Figure 4 shows that the surface tension keeps constant, and the value is as high as 60 mN/m when the G3-to-OD ratio is lower than 6:100, which means that in these cases the polymer is all absorbed at the interface and there is almost no polymer dissolved in water. However, when the ratio exceeds 8:100, the surface tension begins to decrease, which indicates that the amount of the polymer is too much and there is excess polymer in the dispersions. By comparison with the curve of G3 water solutions in Figure 4, we can find that 97% of the polymer is still absorbed by the oil droplets when the G3-to-OD ratio is 10:100. Thus it can be deduced that the capsules are formed effectively by the polymer at this ratio (10:100) and the free polymer dissolved in the dispersion could be neglected. The ratio (10:100) is used to prepare cross-linked nanocapsules in the following experiments.

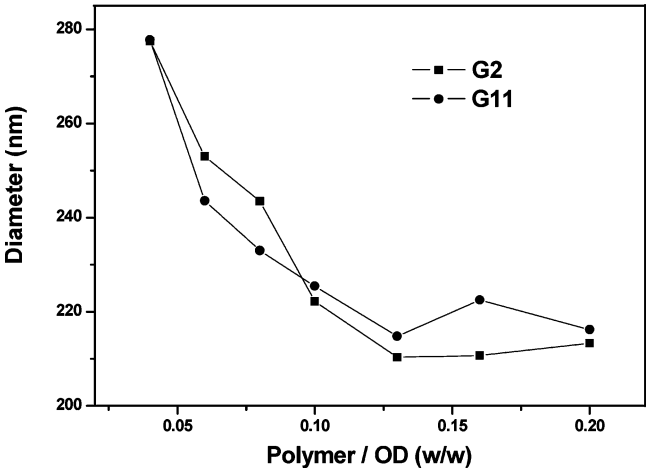

Figure 5. Mean droplet diameters of the miniemulsions prepared with hydrophilic polymers having similar CLA side chains and different hydroxyl group contents.

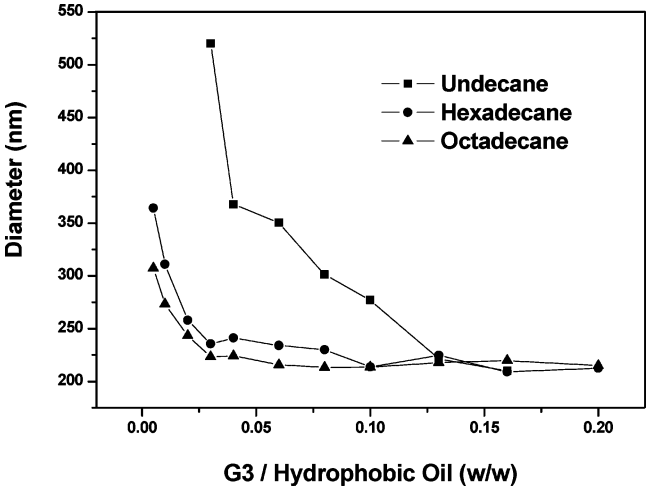

Figure 6. Mean droplet diameters of the miniemulsions prepared with different oils.

Furthermore, the miniemulsions prepared by G2 show similar particle sizes when the polymer amount is sufficient enough, which is further evidence to support our opinion.

Influence of the Composition of Amphiphilic Copolymer on Miniemulsions. The composition of the polymer may play an important role in the formation of miniemulsions. Figure 3 shows the curves of the miniemulsions prepared with G1, G2, and G3 at different polymer-to-OD ratios when the concentration of OD in acetone is kept at 6.4 mg/mL. The standard deviation (error bar in Figure 3) of the particle shows that the differences among these curves are statistically significant. As we mentioned previously, when the acetone solution is poured into water, small oil droplets (ca. 210 nm) are formed immediately, and if the polymer is sufficient enough, then the particle sizes do not change. Figure 3 shows that to prevent the small droplets from coalescing the minimum quantity of G1 is 16% of OD, and that of G3 is only 6%, which means that the polymer with more CLA side chains will provide better protection for the oil droplets. This phenomenon is in agreement with the theoretical results for polymers with multiple binding pendants for colloidal stabilization.[31] The polymers with multiple binding pendants may exhibit a cooperative effect for surface stabilization. In the conditions of fixed chain length, introduction of more binding pendants into the polymer chain may enhance the surface adsorption. We also examined the miniemulsions prepared by G2 and G11, which has similar CLA side chains and different hydroxyl group content on the backbone (Figure 5). It is very difficult to observe significant difference between the curves, which means that the number of the hydrophobic CLA pendants exerts a greater influence on the droplet stabilities than the composition of the main chain.

Polymer G4 with 18.9 CLA side chains is also used to prepare miniemulsions, but it is less effective than G3. It may be attributed to the shorter length of the backbone between two binding pendants, leading to the difficult bending of the PEO main chain.

Influence of Different Oils on Miniemulsions. A series of alkanes such as octadecane, hexadecane, undecane, and heptane are used to investigate the influence of the hydrophobe on minimulsions, and the experimental conditions are the same as those in the previous section. The obtained miniemulsions were stirred for 24 h, and then the particle sizes were measured. As Figure 6 shows, at a low polymer-to-oil ratio such as 4:100, the particle size of the miniemulsion increased as the molecular weight of the hydrophobe decreased, but the diameters of all of the samples are near 210 nm when the ratio exceeds 13:100. In the case of heptane, we did not detect any particles by DLS. For the cases of octadecane and hexadecane, the miniemulsions are still stable after 2 weeks; however the particles disappeared in dispersions prepared with undecane in 2 weeks.

These results indicate that highly water-insoluble oil is needed to prepare stable miniemulsions. The dispersion must be stabilized against molecular diffusion degradation (Ostwald ripening) even if the polymer provides sufficient colloidal stability of droplets. When the small droplets are obtained, there is a statistical distribution of droplets sizes. If the oil is slightly soluble in water, then the oil will, over time, automatically diffuse from the smaller droplets into the larger ones. This is a process of interfacial energy decrease, since the loss in interfacial area of the smaller droplets is greater than the gain in interfacial area of the larger ones. In Figure 6, the size of the particles at high polymer contents is around 210 nm within 24 h even if undecane is used. We think that at high polymer contents the size distribution of the particles is narrow because the polymer provides enough protection to the oil droplet formed in the first process, then the driving force for coalescence is reduced. When the amount of polymer is reduced, more large droplets were formed, and the size distribution of the particles is wider than that in the case of high polymer content, and the coalescence takes place more rapidly. Although the small particles could be prepared and no coalescence is observed even when undecane is used during 24 h, the particles disappear in the dispersions in 2 weeks, which shows that they are not stable even if enough polymers are used. So the stabilities of the droplets are decided by the solubility of the oil in water when the polymer is sufficient. The lower the solubility of the oil in water, the higher the stability of the droplets. Thus in our system, octadecane and hexadecane were the ideal choice.

Cross-Linking of the CLA Chains. G2 or G3, OD, and AIBN are dissolved in acetone and then poured into water with a polymer-to-oil ratio of 10:100. After the miniemultion is obtained and degassed, the temperature is elevated to 70 °C to cross-link the CLA chains. The conversion of the diene group in CLA ($\lambda_{max} = 233$ nm, $\epsilon = 19\,000$ L mol^{-1} cm^{-1}) is measured by UV spectroscopy. When G2 is used, only 52% of CLA is cross-linked although the amount of AIBN is much more than that of CLA. The low conversion may be attributed to two facts: (1) The CLA on the main chain of the copolymers is located only at the interface. (2) The diene groups of CLA are not close to each other and cannot move freely. This low cross-

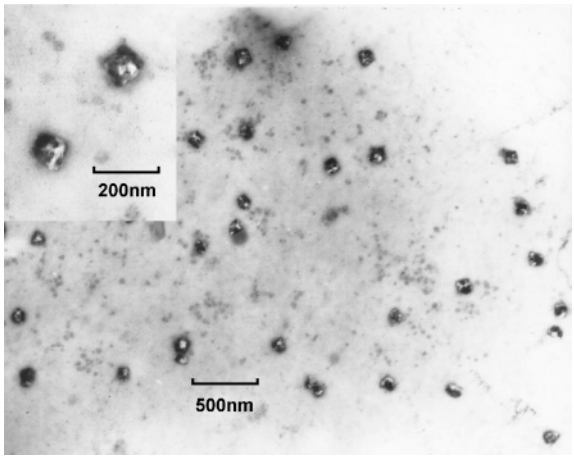

Figure 7. TEM image of the nanocapsules prepared with G2 in the absence of CLA.

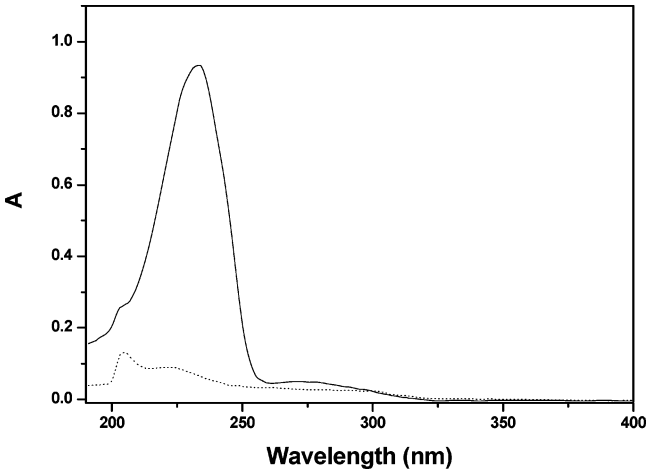

Figure 8. UV spectra of Nc23 nanocapsules before and after cross-linking: solid line, the absorption before cross-linking; dashed line, the absorption after cross-linking.

linking density is also proven by TEM images. From Figure 7 it is observed that the particles are flattened on the copper grid and seem like lamellae, and furthermore, all of the lamellae are cracked. It could be attributed to the low cross-linking density and the thin shells of the particles. In sample preparation for TEM, the shells of the capsules are easily cracked in the drying process, and then the thin shells would be flattened on the copper grid to form cracked lamellae after evaporation of OD in the core. To solve this problem, some free CLA molecules are added to the oil phase to improve the cross-linking density. Thus CLA (5%, 10%, or 15% of the OD weight) is added to acetone solution, respectively, when the capsules of G2 are prepared. After emulsification and cross-linking, nanocapsules (Nc21, Nc22, and Nc23) are obtained, and nanocapsules Nc31, Nc32, and Nc33 by G3 are obtained with the same procedure. The conversions of diene groups are calculated as follows

$$C = ((1 - A_{\text{after}})/A_{\text{before}}) \times 100\% \qquad (3)$$

where C refers to the conversion of the diene groups, A_{after} refers to the absorption of nanocapsules after cross-linking, and A_{before} refers to the absorption of nanocapsules before cross-linking. High conversions (>90%) of the diene groups are achieved within 1 day (Figure 8). The nanocapsule dispersions are stable, and the particle sizes do not change after 5 months.

The TEM image of the nanocapsule Nc23 is shown in Figure 9a, and Figure 9b is its amplified morphology. The hollow

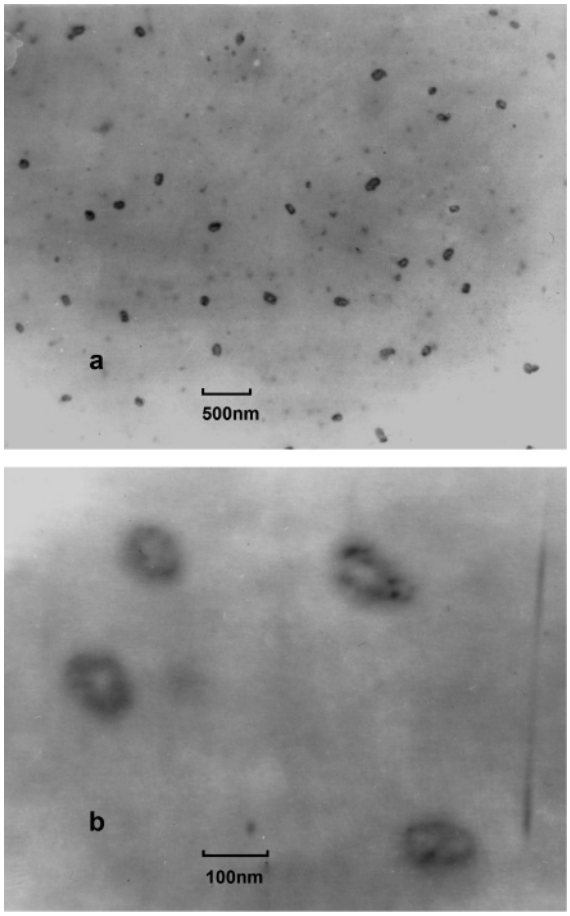

Figure 9. (a and b) TEM images of Nc23 nanocapsules prepared with G2 and CLA. (The CLA weight was equal to 15% of the OD weight.)

structure is clearly observed in Figure 9b. In fact, at first we can only see dark particles in TEM, and then the hollow structure appears within half a minute. It implies that OD is encapsulated in the particle and then evaporated by electron beam irradiation. This phenomenon has also been observed by Scott et al.[15] and used as a proof to demonstrate the oily core of the capsules. The morphology of Nc33 is similar to that of Nc23, and the average particle diameter determined from the TEM images is 131 ± 25 nm (35 particles are measured), which is much smaller than that measured by DLS (ca. 210 nm). Three factors may be responsible for this phenomenon: (1) Light scattering is weighted in favor of larger objects (i.e., it is a *z*-average). (2) The dried particles may undergo a change in volume because the shell structure of the PEO chains is likely to collapse when it was no longer solvated.[32] (3) DLS provides information about the hydrodynamic radius of the particles, which includes the hydrated particle and the surrounding sphere of solvent. The AFM image of sample Nc23 on a mica surface shows that the particle size and shape are consistent with those determined by TEM.

To make sure that the shells are well cross-linked, nanocapsule dispersions of Nc21, Nc22, and Nc23 are condensed at 50 °C under reduced pressure and then dissolved in ethanol. For comparison, an un-cross-linked nanocapsule dispersion of Nc23 (un-Nc23) is treated with the same procedure. These samples are measured by DLS (Table 2). The particle sizes of Nc22 and Nc23 in ethanol are increased to 320.3 and 368.7 nm, respectively, and no particles were detected in Nc21 and un-Nc23 ethanol solutions. These results reflect the effect of cross-linking on maintaining the integrity of the Nc23 shell. When

Table 2. Diameters of Nanocapsules before and after Treatment with Ethanol

sample	D_{water}[a] (nm)	$D_{ethanol}$[b] (nm)
Nc21	210.2	*c*
Nc22	202.4	320.3
Nc23	203.3	368.7
un-Nc23	209.7	

[a] D_{water} refers to the diameter of the nanocapsules in water. [b] $D_{ethanol}$ refers to diameter of the nanocapsules treated with ethanol. [c] No particle was detected by DLS.

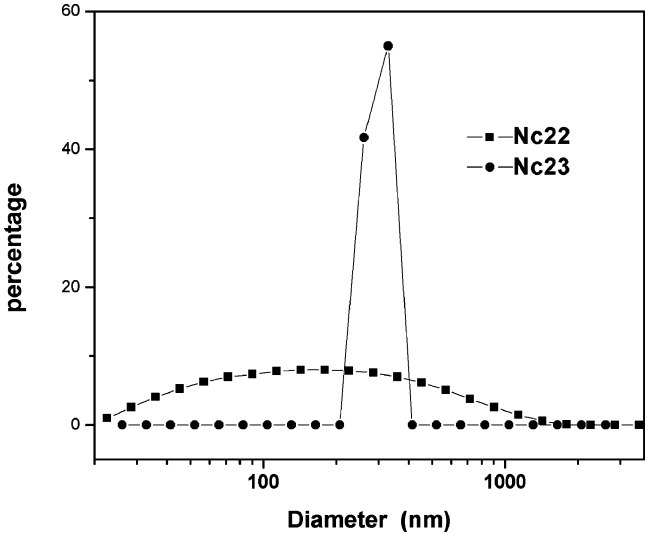

Figure 10. Diameter distribution curves of Nc22 and Nc23 nanocapsules in ethanol.

un-Nc23 is treated with ethanol, it will be dissolved in the solvent, so particles cannot be detected. The DLS results for Nc21 in ethanol show that its cross-linking cannot maintain the integrity of the shell, so the shells are broken into little pieces in ethanol. From diameter distribution curves in Figure 10, the differences between Nc22 and Nc23 in solvent can be found; the diameters of Nc23 are confined to a narrow range, but those of Nc22 expand broadly. It implies that all nanocapsules of Nc23 maintain integrity but some of Nc22 are broken into pieces. This result demonstrates that the cross-linking of Nc23 is more effective than that of Nc22. The increase of the particle size in ethanol may be caused by the removal of the core and the swelling of the shell.

Encapsulation Characteristics of Nanocapsules. Pyrene is chosen as a model compound to investigate the encapsulation properties of the nanocapsules because its contents could be easily measured by UV spectroscopy. Pyrene and OD are simultaneously added to acetone and encapsulated while the capsules are formed. After cross-linking, the capsule dispersions were filtered through a 0.45 μm PTFE filter to remove microcrystals of pyene[33] and then dissolved in acetone/water (v/v, 2:1). The concentration of pyrene is measured by UV absorption spectroscopy at 335 nm ($\epsilon = 4.14 \times 10^4$ L mol^{-1} cm^{-1}). The compound loading content (CLC) and compound loading efficiency (CLE) are calculated as follows

$$\mathrm{CLC} = W_{\text{pyrene loaded}}/W_{\mathrm{OD}} \times 1000 \quad (4)$$

$$\mathrm{CLE} = W_{\text{pyrene loaded}}/W_{\text{pyrene added}} \times 100\% \quad (5)$$

where $W_{\text{pyrene loaded}}$ is the weight of pyrene loaded in the nanocapsules, W_{OD} is the weight of OD, and $W_{\text{pyrene added}}$ is the weight of pyrene added. From Table 3 it could be observed that CLC increased as the amount of pyrene increased, and the CLC varied slightly when the weight ratio of pyrene-to-OD is larger than 1:10, which means that the CLC limited by the volume of the core and maximum content is about 82 mg/g. However, the decrease in the amount of pyrene will cause CLE to increase. High CLE (94%) can be obtained when the pyrene-to-OD ratio is 0.67:10. In comparison with the loading content and loading efficiency of nanoparticles made from a triblock copolymer of PEO and poly(3-hydroxybutyrate) (PHB),[34] the CLC and CLE of our nanocapsules are much higher, which is owing to the liquid core and the high oil content of the capsules. (The maximum loading content and loading efficiency of the PHB-PEO-PHB particles are 6.7 mg/g and 60.9%, respectively. The maximum loading content of our capsule is 66 mg/g when the shell of the capsule is considered.) We cannot find statistically significant changes in capsule size after pyrene loading. We think that the pyrene content is less than 10% of liquid OD, and its effect on particle size is limited.

Table 3. Compound Loading Content and Compound Loading Efficiency of Nc33

sample[a]	OD[b] (mg)	pyrene[c] (mg)	CLC (mg/g)	CLE (%)	$D_{\text{pyrene free}}$[d] (nm)	$D_{\text{pyrene loaded}}$[e] (nm)
Nc33	6.40	1.28	82	41	198.6 ± 2.8	190.8 ± 7.5
Nc33	6.40	0.64	80	80	198.6 ± 2.8	198.2 ± 9.0
Nc33	6.40	0.43	63	94	198.6 ± 2.8	189.6 ± 9.3

[a] The recipe for Nc33 was used to prepare the nanocapsules with pyrene. [b] Weight of OD used to prepare the nanocapsules. [c] Weight of pyrene added. [d] The diameters of the capsule without pyrene. [e] The diameters of the capsules with pyrene loaded.

Conclusion

A new and convenient approach to prepare oily core nanocapsules with PEO surfaces was presented. The shells of the nanocapsules were composed of EO/glycidol copolymers with multiple CLA pendants. The spontaneous droplet formation method was used to prepare miniemulsions. The sizes of the capsules could be easily tuned by varying the oil concentration in acetone. After the CLA side chains were cross-linked, stable nanocapsules were obtained. To increase the conversion of the diene group of CLA, free CLA molecules were added to the oil phase. The obtained morphologies of the nanocapsules by TEM and AFM demonstrated that the shell was cross-linked well. The compound loading experiments of the capsule showed that a loading efficiency as high as 94% could be obtained.

Acknowledgment. We appreciate the financial support of this research from the National Science Foundation of China (Grant No. 20574010)

References and Notes

(1) Zalipsky, S. *Adv. Drug Delivery Rev.* **1995**, *16*, 157−182.
(2) Needham, D.; McIntosh, T. J.; Lasic, D. D. *Biochim. Biophys. Acta* **1992**, *1108*, 40−48.
(3) Torchilin, V. P.; Omelyanenko, V. G.; Parisov, M. I.; Bogdanov, A. A.; Trubetskoy, V. S.; Herron. J. N.; Gentry, C. A. *Biochim. Biophys. Acta* **1994**, *1195*, 11−20.
(4) Zahr, A. S.; Davis, C. A.; Pishko, M. V. *Langmuir* **2006**, *22*, 8178−8185.
(5) Stolnik, S.; Illum, L.; Davis, S. S. *Adv. Drug Delivery Rev.* **1995**, *16*, 195−214.
(6) Hoarau, D.; Delmas, P.; David, S.; Roux, E.; Leroux, J. C. *Pharm. Res.* **2004**, *21*, 1783−1789.

(7) Mosqueira, V. C. F.; Legrand, P.; Morgat, J. L.; Vert, M.; Mysiakine, E.; Gref, R.; Devissaguet, J. P.; Barratt, G. *Pharm. Res.* **2001**, *18*, 1411−1419.
(8) Choucair, A.; Soo, P. L.; Eisenberg, A. *Langmuir* **2005**, *21*, 9308−9313.
(9) Li, S.; He, Y.; Li, C.; Liu, X. B. *Colloid. Polym. Sci.* **2005**, *283*, 480−485.
(10) Rigler, P.; Meier, W. *J. Am. Chem. Soc.* **2006**, *128*, 367−373.
(11) Hillaireau, H.; Doan, T. L.; Appel, M.; Couvreur, P. *J. Controlled Release* **2006**, *116*, 346−352.
(12) Takasu, M.; Kawaguchi, H. *Colloid. Polym. Sci.* **2005**, *283*, 805−811.
(13) Couvreur, P.; Barratt, G.; Fattal, E.; Legrand, P.; Vauthier, C. *Crit. Rev. Ther. Drug Carrier Syst.* **2002**, *19*, 99−134.
(14) Torini, L.; Argillier, J. F.; Zydowicz, N. *Macromolecules* **2005**, *38*, 3225−3236.
(15) Scott, C.; Wu, D.; Ho, C. C.; Co, C. C. *J. Am. Chem. Soc.* **2005**, *127*, 4160−4161.
(16) Tiarks, F.; Landfester, K.; Antonietti, M. *Langmuir* **2001**, *17*, 908−918.
(17) Ni, K. F.; Shan, G. R.; Weng, Z. X. *Macromolecules* **2006**, *39*, 2529−2535.
(18) Antonietti, M.; Landfester, K. *Prog. Polym. Sci.* **2002**, *27*, 689−757.
(19) Zhang, Y. W.; Jiang, M.; Zhao, J. X.; Zhou, J.; Chen, D. Y. *Macromolecules* **2004**, *37*, 1537−1543.
(20) Atkin, R.; Davies, P.; Hardy, J.; Vincent, B. *Macromolecules* **2004**, *37*, 7979−7985.
(21) Liu, F. T.; Eisenberg, A. *J. Am. Chem. Soc.* **2003**, *125*, 15059−15064.
(22) Antonietti, M.; Forster, S. *Adv. Mater.* **2003**, *15*, 1323−1333.
(23) Rodriguez-Hernandez, J.; Checot, F.; Gnanou, Y.; Lecommandoux, S. *Prog. Polym. Sci.* **2005**, *30*, 691−724.
(24) Soo, P. L.; Eisenberg, A. *J. Polym. Sci., Part B: Polym. Phys.* **2004**, *42*, 923−938.
(25) Breitenkamp, K.; Emrick, T. *J. Am. Chem. Soc.* **2003**, *125*, 12070−12071.
(26) Ali, M. M.; Stover. H. D. H. *Macromolecules* **2003**, *36*, 1793−1801.
(27) Fitton, A.; Hill, J.; Jane, D.; Miller, R. *Synthesis* **1987**, 1140.
(28) Li, Z. Y.; Li, P. P.; Huang, J. L. *Polymer* **2006**, *47*, 5791−5798.
(29) Ganachaud, F.; Katz, J. L. *ChemPhysChem* **2005**, *6*, 209−216.
(30) Vitale, S. A.; Katz, J. L. *Langmuir* **2003**, *19*, 4105−4110.
(31) Cao, D. P.; Wu, J. Z. *Langmuir* **2005**, *21*, 9786−9791.
(32) Eckert, A. R.; Webber, S. E. *Macromolecules* **1996**, *29*, 560−567.
(33) Ma, Y. H.; Cao, T.; Webber, S. E. *Macromolecules* **1998**, *31*, 1773−1778.
(34) Chen, C.; Yu, C. H.; Cheng, Y. C. *Biomaterials* **2006**, *27*, 4804−4814.

BM0701797